IEEE Access
Multidisciplinary | Rapid Review | Open Access Journal

Received August 19, 2021, accepted September 27, 2021, date of publication October 5, 2021, date of current version November 2, 2021.

Digital Object Identifier 10.1109/ACCESS.2021.3118283

Development of a Cyber-Physical System to Monitor Early Failures Detection in Vibrating Screens

PABLO AQUEVEQUE[1], (Member, IEEE), LUCIANO RADRIGAN[1], (Student Member, IEEE), ANIBAL S. MORALES[2], (Member, IEEE), AND EDUARDO WILLENBRINCK[3]

[1]Department of Electrical Engineering, Universidad de Concepción, Concepción 4070386, Chile
[2]Department of Electrical Engineering, Universidad Católica de la Santísima Concepción, Concepción 4090541, Chile
[3]Willenbrinck y Cia. Ltda, Santiago 7980265, Chile

Corresponding author: Pablo Aqueveque (pablo.aqueveque@udec.cl)

This work was supported in part by Corporación de Fomento (CORFO) Chile and Programa Tecnológico: Habilitantes en Manufactura Avanzada 18ptecma-102694; in part by the Center for Industry 4.0, Faculty of Engineering, Universidad de Concepción, Chile; in part by Agencia Nacional de Investigación y Desarrollo (ANID), Chile; and in part by Comisión Nacional de Ciencia y Tecnología (CONICYT) Fondo de Equipamiento Mediano (FONDEQUIP) under Grant EQM150114. The work of Luciano Radrigan was supported by ANID through the Scholarship ANID/Becas de Doctorado Nacional/2021-21210655. The work of Anibal S. Morales was supported by the Project Grant FIAEC N°1 Universidad Católica de la Santísima Concepción (UCSC), Chile.

ABSTRACT Vibratory screens are used in mining to classify mineral and send it to different pathways, normally using conveyor belts. Vibration analysis techniques are commonly used for condition monitoring and early detection of unforeseen failures to generate predictive maintenance. This paper proposes a novel solution to implement wireless sensors forming an instrumentation dedicated network combined with data-driven machine learning for monitoring vibrating screens. The system is optimized explicitly for vibratory equipment, which sets it apart from general-purpose condition monitoring systems. Embedded sensors are battery-powered and robust to withstand constant vibratory movement. The data used for training the machine learning models are gathered from a lab setup and discrete element simulations. The test bench consisted of a lab-scale vibratory screener, in which 3-axis accelerations, cumulative damage and wear are measured using sensors embedded in the rubber screens. Proposed data-driven machine learning models classify each screen condition in states according to the ISO 2372 standards for vibration severity. The system can identify random failures (based on test bench measured data) as progressive degradation failures over time (based on discrete element methods simulation results). The accuracy of the classification algorithms consistently ranges from 95% to 98%. Moreover, the system allows the early detection of unacceptable states up to 168 hours before the screen's end-of-life predation by an expert. The system is characterized for (i) avoiding unplanned downtime and consequently (ii) increase operational availability. The system is intended to notify users when an abnormal operation is detected and impending failure events in the early stage.

INDEX TERMS Industrial Internet of Things, mining, vibrating screen, data-driven, condition monitoring, embedded sensors.

I. INTRODUCTION

The classification of solid material according to its size is a stage of many industrial processes. Granulometric classification is important in mining processes since it is directly related to its efficiency. If the material does not comply with the specific granulometry, it must be crushed again [1].

Vibratory screeners are industrial machines used to sort aggregates through their high-intensity accelerations. Used intensively in mining operations, they can screen thousands of tons of material per hour. These machines comprise several decks of screens (or screen panels) with multiple holes of a specific size that classify the material according to the process's requirements. The material is typically classified to have a diameter less than 100 [mm] since at a larger size the downstream process becomes inefficient [2], [3].

The associate editor coordinating the review of this manuscript and approving it for publication was Ming Luo.

As the mining industry is automatized, it becomes necessary to monitor and forecast critical machine operational conditions. Condition-based maintenance, or predictive maintenance, is a decision-making strategy that uses condition monitoring information to optimize critical machine availability [4].

Condition Monitoring (CM) enables early detection of failures to reduce downtime and operating costs, facilitates proactive responses, and improves productivity, reliability, availability, and maintenance of critical equipment [5], [6]. Unexpected breakdowns cause unplanned downtime and production losses [7].

A critical machine is defined as a crucial machine for the operational continuity of a process. Criticality is a relative measurement of the consequences of a failure mode and its frequency of occurrence [8]. Failure criticality corresponds to the product of its frequency and its impact. The failure frequency corresponds to the number of failure events that occur in a given period, and the failure consequence refers to the result of stopping the equipment under evaluation; consequently, we can classify the vibratory screen as critical machinery [9], [10], [2]. The vibratory screen components that present a high failure rate are exposed to cyclical loads leading to fatigue failure. The most common maintenance problems are related to the spring system, wear of screens, bearings, shock absorbers, belt loosening, and electrical failures. Mining maintenance practice shows that the main downtimes of vibrating screeners account for 10% to scheduled maintenance and the remaining 90% to unscheduled stops due to unforeseen failures. Table 1 shows the most common faults [11].

TABLE 1. Frequency distribution of unplanned downtimes in vibratory screeners.

Type of downtime	%
Structural system failures (include screen panel loose)	32%
Troubleshooting interruptions due to Operational issues (include blockage and clogging loss)	12%
Motor drive system failures (include motor coupling breakdown due to excessive Deck unbalance)	12%
Another type of failures (include screen panel breakdown)	24%
Electrical system failures	20%

Two main research topics can be identified in the state of the art of condition monitoring solutions for vibrating screen: (*i*) Development of simulation models based on discrete element methods (DEM) for characterization of operation and maintenance; and (*ii*) Time-frequency analysis of measurement data collected in a specific time window with commercial instruments. The literature review indicates the research area (*i*) is used to improve equipment designs. Most references in the research area (*ii*) focus on developing new algorithms for the diagnosis of the equipment state [12]–[15].

This paper explores data-driven methods to estimate the vibrating screen's fault condition and health status using a novel design for wireless accelerometer and wear sensor modules embedded in deck screens for online condition monitoring. In addition to developing small, low-energy electronic components support industrial operating conditions for monitoring applications and mining equipment. This document aims to develop algorithms for early fault detection using machine learning techniques. The enhanced capabilities of proposed real-time condition monitoring system surpass the standard technology practice for early fault detection in vibratory screeners in mining.

Specifically, the proposed system consists of a plurality of wireless sensors forming an instrumentation dedicated network combined with data-driven machine learning to monitor vibrating screens. Each mining vibratory screener is typically composed of one to three decks, each composed of 96 or more rubber screens. Vibratory screens are disposable components by design. Lifespan of screens typically ranges from 30-60 days. In proposed monitoring systems, each screen contains an embedded electronics module with dedicated sensors (accelerometer and wear measurement sensors) and a wireless communication module. The embedded sensors comprise physical sensors, signal conditioning electronics, a low-energy consumption microcontroller, power management unit and WiFi IEEE Std.802.11n communication module. The embedded sensor modules communicate with a local server using a dedicated WiFi star-topology network accessed via a web platform for operation and maintenance (O&M) analysis purposes on-site. Different data-driven machine learning algorithms run at local server level to predict machine health status based on machine working time, screen wear, and vibration severity collected from real-time sensor information.

This work provides a rugged hardware (with customized firmware) that is completely embedded in the Deck's rubber screens, forming the first Smart-Deck solution for vibratory screens. The Smart-Deck design reliably acquires data in real-time from the vibrating screens. Machine learning models subsequently diagnose the machine's condition (with greater than 90% accuracy). The design of hardware, firmware, software and data-driven models was carried out to cover the vibratory screener technical requirements for O&M. Correspondingly, features like high energy autonomy (exceeding screen lifespan), reliable sensor measurements and robust wireless communication are key for the proposed solution. A low-energy consumption hardware design is proposed for wireless sensors. Also, IP67 protection is considered for embedded sensor modules to endure the harsh mining operating conditions. The embedded electronics module is light and small size to ensure ease of integration into rubber screens and avoid operational or maintenance issues.

This paper addresses the following challenges for condition monitoring: (*i*) how to acquire reliable data from the lab setup (by simulating the operation of a real vibrating screen) in real-time adequately, and (*ii*) how to use gathered data to train suitable machine learning algorithms to detect random failures and to predict individual vibratory screen

wear related failures. The condition monitoring system proposed enables early detection of cumulative damage, random failures and condition-based maintenance of the machine.

II. VIBRATORY SCREENS

A. CLASSIFICATION CHARACTERISTICS

Since the classification process is probabilistic, it is not 100% efficient. In ideal processing conditions, the vibratory screener must provide passing and increase the probability for the particles to penetrate the screen holes to maximize the processed the tonnes per hour and consequently the classification efficiency. To ensure a good classification of the material, the operational parameters must be controlled considering the following factors [16], [17]:

- Hole Size: there is a high probability that the material particles penetrate into the screen holes if they do not exceed 50% of the hole size; If the particle is almost the same size as the holes, likely, it will not pass through the holes.
- Geometry of material: the vibratory screener classifies material in two dimensions, but the particles have three dimensions. This introduces challenges for the sorting process, causing some particles with only one dimension meeting the hole's size to be rejected by the deck screen. Consequently, for a particle to pass through screen holes, at least two of its dimensions must be less than the holes' size.
- Distribution: vibratory screens do not classify the particles individually but rather a group of particles that compete with each other to pass through the holes in the screen deck.
- Velocity: as particles travel over the Deck, they speed up, making it difficult to pass through the screen holes. The longer the residence time of particles over the screen holes, the more likely they are to pass through them.

After the comminution in primary crushers, the material is classified according to its size. The classified material by vibratory screeners must comply with maximum size requirements for the downstream processes (mill and concentration). Any failure in screeners in primary, secondary or tertiary crushing stages can overload downstream crushing stages, produce bottlenecks, process queuing, and delay upstream and downstream. See Fig. 1.

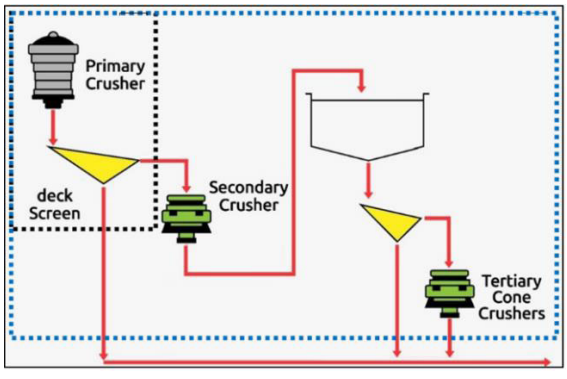

FIGURE 1. Primary, secondary and tertiary crushing stages & primary and secondary vibratory screening stages.

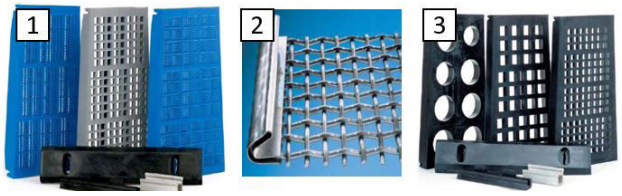

FIGURE 2. 1) Polyurethane screen, 2) Steel screen, 3) Rubber screen.

B. OPERATING CHARACTERISTICS AND TYPES OF PROBLEMS IN VIBRATORY SCREENS

there are seven main factors in the classification process that affect the particulate material screening capacity and efficiency, these are: (i) Higher percentage of mean feed size, (ii) Lower percentage of feed, (iii) Wet material, (iv) Slotted holes, (v) Excessive moisture in material, (vi) Elongated particle shape, (vii) Material size close to screen hole size.

The material classification process is carried out through the deck screens, which have multiple holes that define the maximum particles size that get a free pass through them. The screens are subjected to progressive wear due to friction (generated by the material when moving and rolling over the Deck), so it is necessary to perform maintenance periodically [18].

The screens can vary in size and manufacturing materials. They can have different uses and mechanical behaviors depending on their specific designs [19], [20]. Figure 2 shows the different types of screen

- Wire grids: they are manufactured using steel and are characterized by having a high resistance. However, these types of screens corrode easily when exposed to humidity, which is a significant limitation. A common practice is run screeners with wet material to improve the flow and tonnes per hour in classification.
- Plastic (monofilament and polyurethane): wet particles can be separated from the material without corrosion. One of the significant problems of this type of screens is that they break easily when subjected to high mechanical stress.
- Rubber: screens that exhibit a high elasticity and can withstand high mechanical stress under typical operating conditions

The main operational problems that arise in deck screens are the blockage by particles [17]:

- Blockages by particles with a size equal to screen hole size that get stuck and block the passage of other particles or finer particles.
- Blockages caused by several small particles that arrive at screen hole simultaneously, resulting in a bottleneck that blocks particle passes, despite being smaller than the holes.
- Blockages caused by fine particles with a high moisture content that produce adhesion and clogging.

C. DYNAMIC CHARACTERISTICS

The mechanical systems of the screens can be described in terms of its their degrees of freedom. Each degree of

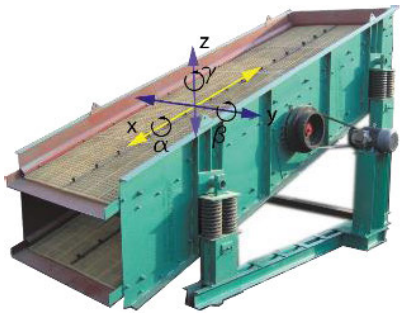

FIGURE 3. Degrees of freedom Deck [21].

freedom has associated a natural frequency and therefore, a way of vibrating. Fig. 3 shows a vibrating screen as observed with its degrees of freedom. The x, y, z axes correspond to longitudinal axes and the α, β, γ to the torsional axes, which correspond to the vibratory system's angular deformations [17], [21].

Table 2 shows a summary of the root causes of typical vibratory motion problems due to changes in dynamic response parameters of the screener. The manufacturing materials, dimensions, and quantity of individual screens per vibratory Deck directly impact the stiffness and the total mass subjected to vibratory motion. These factors affect the balance, vibrating modes and the natural resonance frequency. Damage of springs in the supports of vibratory screeners also results in an unbalanced operation.

TABLE 2. Root-causes of vibratory motion problems.

Cause	Consequence
Springs installed unevenness.	Lateral overload
Springs broke or wear.	Overload
Loose clamps.	Blockages deck
Accumulation of material on deck screens	Particle velocity

III. CONDITION MONITORING OF VIBRATORY SCREENS

Today, there are several monitoring systems for vibrating screeners available in the market. The condition monitoring is carried out using acceleration, temperature, and strain gauge sensors fixed to the vibrating screener structure with these systems. Once the data is collected, expert knowledge and physics based models are used to evaluate the condition of vibratory screener.

The experience-based models approach is typically generated by gathering the accumulated knowledge among experts in fuzzy logic. With these models, measurements combined with experience leads to a possible corrective action. Experience-based approaches can be an efficient way to transfer knowledge to a large group of end-users of equipments but rely on experts' existence within the area. The main benefits and drawbacks are as follows: (*i*) the rules are typically easy to understand, (*ii*) the process is logical from a human point of view, (*iii*) there is a risk of combinatorial explosion for complex systems with numerous failure modes, making the approach complicated even though the individual rules are easy to understand, and (*iv*) it requires experts with deep system knowledge.

The physics-based models employ first order principles and use the underlying physics to explain both the operation and the various degradation processes of a system. The main benefits and drawbacks are as follows: (*i*) the models incorporate physical understanding and empirical curves, (*ii*) the models can be transferred between similar assets, possibly requiring new parameter tuning, (*iii*) The approach requires accurate physical models of fast dynamics, (*iv*) detailed knowledge and models of slow degradation are needed, (*v*) model development is often hard and time consuming, and (*vi*) the physics based approaches easily become complicated.

It should be pointed out that none of described model approaches are able to capture unknown failure modes. Also, with experience based models, sometimes arise the need for complimentary physical models of degradation and dynamics to improve the condition monitoring accuracy and/or precision [22]–[24].

Examples of OEM/OTM vendors that provide condition monitoring applications through data acquisition with sensors can be found in [25], [26]. Functionality of these technology-based-applications are quite similar. The solutions consist of sensors bolted or attached temporarily to the vibrating screener structure to measure vibrations excursions and communicate either by wire or wirelessly with a local application server. Measured data is stored and processed to provide equipment status regularly through different human-machine interfaces. See typical solution architecture in Fig. 4 [27]. The main difference between solutions are the characteristics of sensors deployed. Technical specifications vary in type, size, measurement accuracy, and price according to process operating conditions.

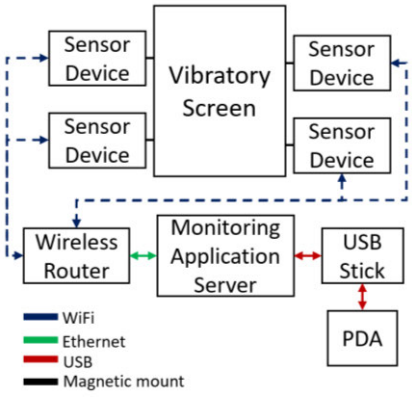

FIGURE 4. Diagram of the monitoring system for screens [27].

Table 3 shows a feature comparison between a number of existing commercial OEM/OTM solutions for vibrating screener monitoring. These systems use a plurality of sensors,

TABLE 3. Commercial solutions for vibratori screen.

Item \ Solution's Company	System 1 [57]	System 2 [58]	System 3 [59]	PROPOSED SYSTEM
On-line Detection Deck Blocking	No, the system monitors the mechanical and structural operational condition of the vibratory screen.		No, the system can only identify the occurrence of numerous simultaneous blockages.	Yes.
On-line Unbalanced Load Detection	No, the system can only identify high levels of unbalance in deck load, it does not monitor operational condition of individual screens.			Yes.
On-line Random Deck Failure Detection	No, the system monitors the mechanical and structural operational condition of the Deck.		No, the system can only identify the loss of multiple neighboring,	Yes.
Performance Classification On-line	No, the system only monitors the mechanical and structural operational condition of the screen, the system does not have the ability to estimate the online classification performance.			Yes

typically temperature and accelerometers to perform condition monitoring. All solutions covered in Table 4 use empirical control curves based on empirical physics models and experience-based models. These control curves are used to trigger failure alarms using fixed thresholds according to the machinery's condition variables for maintenance diagnosis.

The analysis shown that an opportunity for R&D in condition monitoring systems for vibrating screeners still exists. A number of technology gaps were identified as mandatory to reach the TRL level and the condition monitoring performance demanded by the application. State-of-the-art condition monitoring capabilities need to be improved to detect additional process random and progressive degradation failures, not covered by existing systems. These additional early-failure detection capabitities include: (*i*) detection of screen panel loose, (*ii*) detection of blocking and/or clogging of screen panels, (*iii*) detection of screen panel breakdown, and (*iv*) detection of excessive Deck unbalance.

With aim to close identified technology gaps, this work proposes a number of technology developments: (*i*) new design of screen panels with smart sensor modules embedded, combined with (*ii*) customized data-driven models for condition monitoring, diagnosis and prognosis.

Challenges to develop new smart screen panels consider: (*i*) light and small size sensors, (*ii*) manufacturing methods to embed sensors into the screens, (*iii*) high energy autonomy of embedded electronics, (*iv*) smart wireless communications, and (*v*) suitable IP protection to withstand harsh environmental conditions, shock and constant vibration.

Data-driven models relieve the need for physical understanding by using measurement data to find the relationships between sensor signals and damage. A review of data-driven statistical approaches is given. Typical benefits are: (*i*) there is no need for physical models of degradation and dynamics, (*ii*) the approach can capture unknown failure modes, and (*iii*) the available techniques are not specific to a certain domain, i.e., the methods can be transferred to different applications. Data-driven approaches addressed in this paper contain both statistical and machine learning techniques. It should be noted that techniques have different requirements to achieve adequate operation of prediction models. Some techniques demand heavy computational time while others require considerable amounts of historical data to perform prognosis. These requirements limit the applicability of these techniques to real-world implementations for real-time prediction.

Heavy historical data requirement is not desirable for the application since historical data is not always available or well labelled. The use of unreliable and/or low-quality data results in unreliable, inaccurate forecasts. It causes false alarms and unnecessary machine downtime. On the other hand, heavy computation time can be avoided using modern powerful multi-core computers/servers and cloud computing. Despite the processing hardware available on premise or in the cloud, the most suitable algorithms for the application will be the ones with moderate data required to ensure real-time operation when scale-up the number of machines being monitored.

Considering the design boundary conditions of data requirement and computation time, the best machine learning algorithms for the application should not require a significant computational capacity, must be able to provide good equipment condition predictions using small datasets with limited historical information content for training, and be easy to implement as industrial monitoring systems.

IV. SOLUTION DESCRIPTION

The proposed system is a comprehensive solution that comprises hardware and firmware for data collection and software for O&M data analysis of vibrating screens.

Each vibrating screen represents an elasto-plastic device, consequently, it has its own vibratory patterns, which can help detect the machinery's health status in real-time [28]. The proposed solution uses a wireless data acquisition system composed by accelerometers and height wear sensors embedded in each vibrating screen panel. The solution requires sensing the vibrating screen in a non-invasive way to obtain accelerations and wear signals during normal operation in

real-time. The sensor modules embedded in rubber screen panels (forming the SmartScreen devices) uses a dedicated WiFi wireless network for data transmission. The SmartScreen sensor network receive and send information from the vibrating screens to the local application server, and vice versa. The proposed solution uses WiFi due to the high data traffic between the SmartScreen (more than 100 units) and the server during a very short time. In addition, through implementing a TCP / IP socket, the delivery of data packets is guaranteed. Other more energy-efficient solutions such as Bluetooth and Zigbee cannot establish stable communication with a high number of sensors, considering that the sensor is embedded in the rubber. Over the Deck, there is constant material inflow, and their bandwidths are quite limited [29]–[31]. The application server is responsible for three main tasks: (1) store measured values generated by the sensors embedded in each screen panel into a database; (2) host the control, configuration, and monitoring software of smart screen panels; and (3) manage measured data, run predictive maintenance models, and backup real-time information into a cloud server for IT/OT and user visualization platforms integration purposes [32].

Figure 5 shows the components of the proposed condition monitoring cyber-physical system.

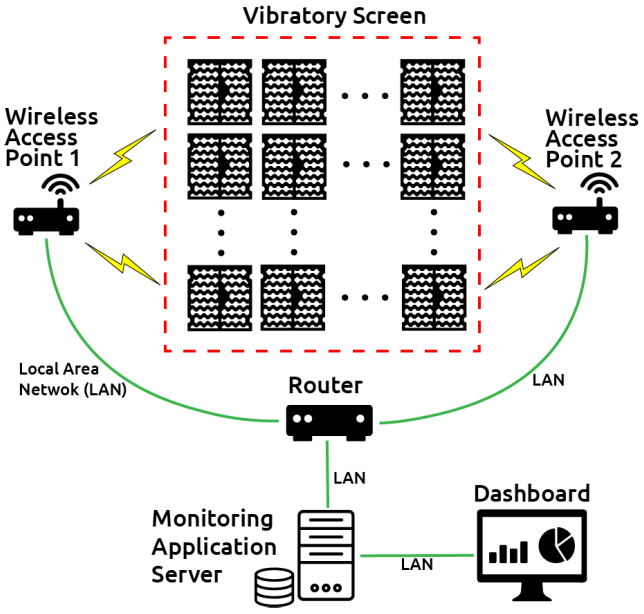

FIGURE 5. Diagram of the proposed screen monitoring system.

The proposed cyber-physical system has a functioning that is composed of 6 main stages. Figure 6 shows the functions of the system in a flowchart format. The multiphysics system will provide the operators and maintainers with indicators associated with the vibratory screen operation, such as: (i) Diagnostic status, (ii) Early detection of failures, (iii) Forecast horizon for change in operating status. With these indicators, workers can take preventive measures to extend the remaining useful life (RUL).

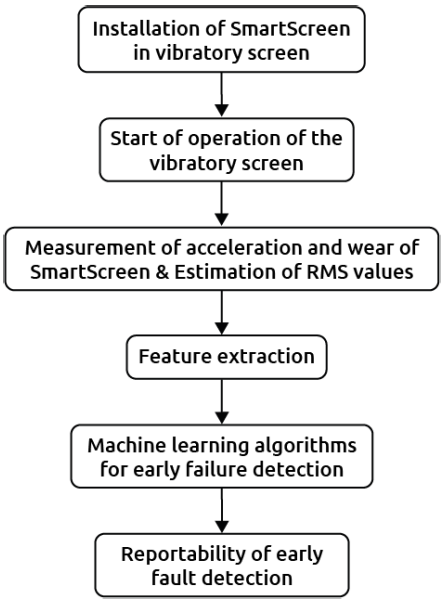

FIGURE 6. Functions of cyber-physical system.

A. SmartScreen SENSOR DESIGN

The SmartScreen Sensor design considers the following embedded capabilities: data storage and processing functionalities, wireless communication, 3-axis inertial measurement using accelerometer, screen panel height wear sensor, power supply, and power management unit. Fig. 7 shows the SmartScreen Sensor device functional diagram.

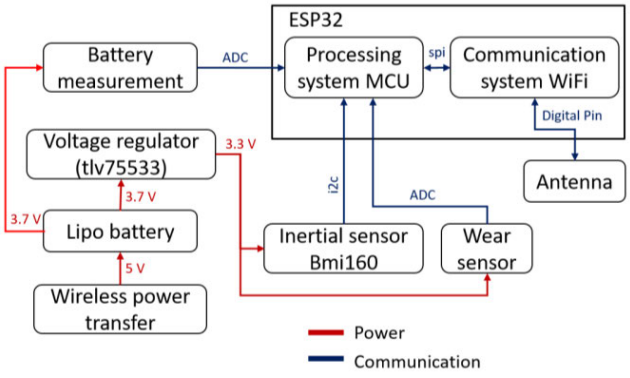

FIGURE 7. Diagram of the monitoring system for screens.

1) PROCESSING SYSTEM

Its function is processing and managing the vibration and wear signals coming from the IMU sensor (Bosch BMI160) and customized wear sensor developed. Thus, the system achieves a total frequency range of 1-500 Hz for inertial signals measurement up to 16g and information from a wear sensor that comprises an electric circuit supported on a substrate. This circuit comprises a plurality of discrete elements wich are coupled in parallel with each other across conductive rails. This wear detection circuit is electrically connected

with a ADC measuring device. The measuring device measures the variability of the resistance. The wear sensor is disposed of adjacent to the central inner wall of the internal frame of each screen panel, which is subject to wear and wears with the object. As the sensor wears, the elements are sequentially decoupled from the circuit, thereby changing the characteristic measured by the device. This change indicates the amount of wear of the vibratory screen panel in the height side.

The amplitude resolution of the accelerometer is 0.01 [G]. This functionality is integrated in the proposed desing as a tool to activate the SmartScreen sensors and put the smart panels in service in the field.

For the implementation of the battery measurement, a voltage divider is used. The voltage dividerh is connected between the battery and an MCU analog-digital converter. The voltage divider uses two 10MΩ resistors in format surface-mount device (SMD) with package 0402.

2) RF COMMUNICATION SYSTEM

This functional block is responsible for the data transmission of estimated parameters of wear and inertial signals measured by the SmartScreen sensor to the server using WiFi. This wireless link also is intended to send configuration parameters to each SmartScreen sensor. The SmartScreen sensor uses a Transmission Control Protocol (TCP) client that communicates with a TCP server hosted on the local server. TCP is used to ensure the reception of measurement data packets. Also, a SQL database is hosted on the local server. The database stores the configuration information of the SmartScreen sensor and the data of the measurements received in the TCP server. The system has standard libraries associated with the development environment, such as custom libraries of appropriate design for the application. The sensor is programmed in C in a Free-Real-time operating system (FreeRTOS) environment. Figure 8 shows the standard functions that the operating system contains. In addition, specific functions were added, such as:

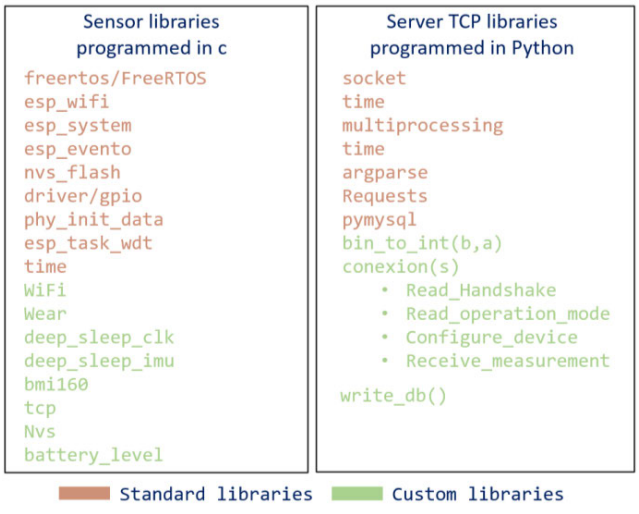

FIGURE 8. Draw software packages.

- WiFi: Manage the connection to the WiFi network. Save the assigned Internet Protocol (IP) and handle protocols for connection errors.
- wear: Discretizes the voltage delivered by the wear sensor and quantifies it in 5 levels.
- deep_sleep_clk: Manages deep sleep mode, with a wake-up controlled by the internal clock.
- deep_sleep_imu: Manages deep sleep mode, with a wake-up controlled by the anymotion function of the BMI160.
- bmi160: Contains the operating functions of the BMI160 sensor. Among these functions, the initialization of i2c communication, sensor configuration, reading of measurement register.
- tcp: Contains the functionality of the TCP client service. The IP and the TCP server port are set.
- nvs: manages writing and reading of non-volatile memory.
- battery_level: Discretizes the voltage delivered by the battery sensor and quantifies it in percentage of charge.

Also, figure 8 shows the standard functions that the Server TCP hosted in local server contains. In addition, specific functions were added, such as:

- bin_to_int: Function that transforms data of type integer (int), into data of type Bytes.
- Connexion: This function will administer a subset of functions associated with connecting the client and the TCP server. The functions that are highlighted are (i) verification of the handshake, (ii) verification of the operation mode of the sensor device, (iii) Configuration of the sensor device, (iv) reading of the measurement data that the sensor device sends to the server TCP.
- write_db: Function that writes the information received from the sensors in the database.

3) POWER MANAGEMENT SYSTEM

An embedded 3.7V 1200mAh LiPo battery is used to power the electronics embedded into each SmartScreen sensor. Also, the proposed design considers a battery wireless recharging feature. The wireless power transfer (WPT) uses an inductive link in the series-parallel topology. The inductive link's operational frequency is 1MHz. The receiver coil is fabricated in a rigid PCB and has a diameter of 15.5 mm, an inductance of 0.85 μH, and resistivity of 486 mΩ. For the rectification proposes its use full-wave rectifier with a DC capacitive filter. Finally, the system use a MCP7383 LiPo battery charger regulator

B. SENSOR SYSTEM IMPLEMENTATION

1) ELECTRONICS SYSTEM

A prototype of the SmartScreen sensor embedded into the vibratory screen panels was implemented for functional performance testing and evaluation. During lab testing, power consumption measurements were accomplished using

Fluke 287 multimeter and the TDS1002C-EDU Tektronix Oscilloscope.

The test protocol for inertial measurements was as follows: (*i*) activation, (*ii*) the sensor starts to measure inertial signals, (*iii*) then establishes a WiFi link with the application server, (*iv*) sent of configuration parameters, (*v*) run a measurement cycle, and (*vi*) after the sensor completes a measurement cycle, it goes into deep sleep mode (until a new measurement cycle need to be performed according to the sampling frequency configured, i.e., every 10-15 minutes). Fig. 9. shows the SmartScreen power consumption measured. The stages of the test protocol are represented by "1", "2" and "3", for deep sleep mode, measurement mode and communication mode, respectively. The wear rate of vibratory screens is different from a mine site to another. It depends directly on the material's geological and mechanic characteristics that are processed, utilization, loading quality, and operating conditions. Typically, the deck screen panels used are replaced every 25-30 days in copper mining, and every 90 days in gold mining. The proposed system considers seamless integration of SmartScreen in the mining operation to avoid operational and maintenance problems and interruptions. The solution is designed to last in service as much time as possible without battery recharging, exceeding the vibratory screen lifespan. The wireless battery recharging capability is included to repleting energy after extended storage periods before installation. It does not represent the primary energy source. The average energy consumption during the measurement and communication stage v) of the system integrated in the vibrating screens is 265 [mW].

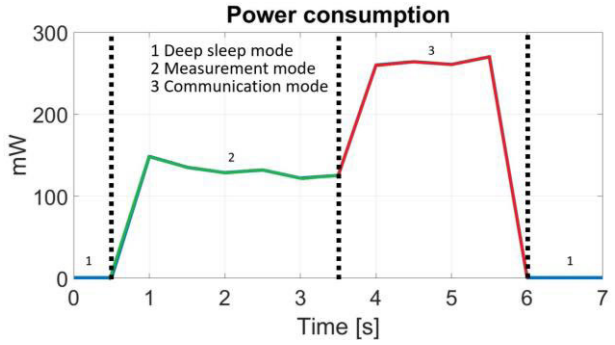

FIGURE 9. Power consumption of SmartScreen sensor during the tests.

Each activation cycle for the vibratory screen measuring last for 5-6 seconds. In each monitoring cycle, the SmartScreen sensor measures the accelerations signals (at 400 Hz sampling frequency), the wear level, the battery charge level, establishes a connection with the application server using a dedicated WiFi network, next connect to a TCP socket, and send all gathered information to the server for further processing and store in database and running the predictive condition monitoring models.

Considering that the sensor: (i) is active (in states 2 and 3 of figure 9) an average of 6 seconds every 15 minutes, (ii) the average consumption of states 2 and 3 (see figure 9) is 60 mA, (iii) the average consumption of state 1 (see figure 9) is 0.02 mA, and the device is always in this state, except when it measures and sends the information. The number of measurements that can be performed with a 1200 mA battery is estimated as follows:

$$\mathrm{Sdt} = \frac{\mathrm{Bpc}}{(\mathrm{Asr} * \mathrm{Acs}) + (\mathrm{Sr} * \mathrm{Cs1})}$$

where:

- Bpc: battery power capacity, in milli ampere hour
- Acs: Average consumption signal 2 and 3 Fig. 8, in milli ampere
- Cs1: Consumption signal 1 Fig 8, in milli ampere
- Asr: Average sensor runtime in signal 2 and 3 Fig 8, in hours.
- Sr: Sensor runtime in signal 1 Fig 8, in hours.

Replacing the values, we obtain:

$$\frac{1200mAh}{\left(\frac{6}{3600}h * 60mA\right) + \left(\frac{3594.5}{3600}h * 0.02mA\right)} = 11764h$$

Considering that the sensor will measure and send information 96 times one day, approximately 122 days of operation are obtained.

2) MECHANICAL SYSTEM

To ensure an IP67 protection against harsh environment conditions in mining, and withstands shock and constant vibration, the electronics of the SmartScreen sensor is embedded into a block of epoxy resin of 30 × 50 × 15 [mm] size. Fig. 10 shows the position of the SmartScreen sensor embedded in the vibratory screen panel. Fig. 11 shows a prototype of the sensor module.

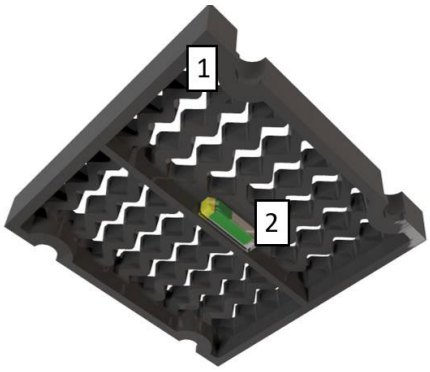

FIGURE 10. Figure 3D showing the position of the SmartScreen sensor embedded in screen rubber. 1- Rubber screen, 2-Sensor position.

C. DATA PROCESSING

The vibratory signals and the wear level measured by the SmartScreen sensor in each monitoring cycle are stored temporarely in the device using a customized data packet. The data packet is sent to the TCP Socket hosted in the application

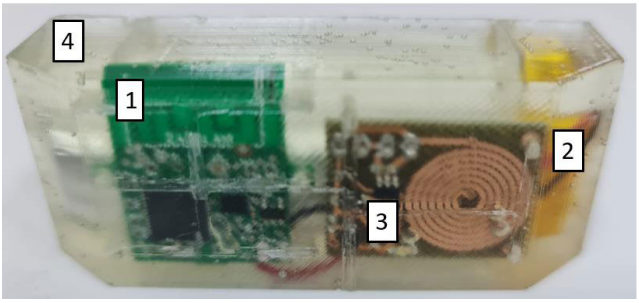

FIGURE 11. Electronic system embedded in resin that forms the SmartScreen Sensor prototype. 1-Electronic measurement and communication system, 2- lipo battery, 3- Wireless charging system, 4- Resin protection.

server at the end of each monitoring cycle. Server daemons save the received data on a TCP socket in a SQL database. The RMS value and the FFT transform are calculated using the measurement time window with acquired vibration signals. Because the present investigation is an exploratory study, it is decided that SmarDeck sends raw data, all triaxial accelerations, to the server. Subsequently, the server estimates the indicators as RMS or variables in the frequency spectrum. This methodology compares the proposed algorithms using the time series of the raw data with the time series of the indicators.

D. HEALTH STATUS DETECTION ALGORITHM

This research proposes a cost-effective solution to implement a monitoring system for vibratory screens with wireless communication and data-driven machine learning capabilities. The 3-axis accelerations and wear discrete level are measured using sensors embedded in the rubber screens during the vibratory screen operation. The deck screen panels accelerations (amplitudes and frequencies) are measured in two different frequency spectra to improve each sensing location's temporal resolution. Proposed data-driven machine learning models classify the wear status and the vibratory motions of the screen panels according to ISO 2372 standards for vibration severity into Good, Acceptable, Unsatisfactory, or Unacceptable categories.

The Good state indicates that the vibratory screen is working in conditions that do not impair asset lifespan. The Acceptable state indicates work conditions in which the screen panel's useful life is not significantly reduced. The Unsatisfactory state indicates that the screen can operate for a limited period in the current operating condition until corrective action arises. The Unacceptable state indicates that the device will suffer a critical failure in short; maintenance is mandatory immediately.

The machine learning algorithms chosen for machine health status classification during vibrating screen operations are Naïve Baye and Support Vector Machine (SVM). These two algorithms were tested considering a prior optimization process of methods parameters, kernel, support, and type with different combinations to achieve a better possible classification.

The protocol to train the machine learning algorithms was the following:

1) Test an algorithm with default parameters.
2) Change the kernel and choose the best.
3) Change support.

These algorithms are explained in the "Diagnostic Algorithms" section.

V. TRAINING DATASETS

The method proposed for detection of failures in vibratory screens is based on data-driven models where datasets are required for training purposes.

This section presents the methodology associated to data-generating process (DGP) using two complimentary modeling methods to improve early failure detection for predictive maintenance in vibratory screeners. The first method uses a test bench, which replicates the operation of a vibratory screener at lab-scale. The tests carried out on the test bench allow the characterization of the frequency spectrum of the accelerations of the vibratory screens without load under different vibrational excitations. The second method consists on the simulation of a vibratory screener under different load conditions using discrete element method software.

A. TEST BENCH DATA-GRENERATING PROCESS

The proposed test bench is made up of three main components. The first component is the stainless steel structure that mimics the inclined plane of a vibrating screen. The second component is the Deck of vibrating screens, which performs the material classification through the rubber screen panels with specific size holes. The third component is the electromechanical excitation system, which allows the test bench vibrates under controlled frequency and amplitude.

The main structure consists of a rectangular base of 125×80 [cm] that supports an inclined plane projected with a height of 57 [cm]. The test bench uses a mechanical isolation system, which is made up of four springs. A three-phase motor is used to perform the controlled vibratory excitation test bench. This motor has a power of 0.52KW and reaches 1000 revolutions per minute. A variable frequency drive is used in the test bench.

Implemented test setup consists of six rubber vibratory screens (that compound the SmartScreen prototype) connected using WiFi via an ASUS RT-AC1200 router to the application server. The application server is implemented in a minicomputer, with Fig. 12 shows the implementation of the test bench in the laboratory environment.

Three different sets of tests were carried out on the test bench as a part of the data-generating process for characterization of real vibratory screen panels: (*i*) excitation of the vibratory screener structure with impulse signals; (*ii*) excitation of the structure with frequencies ranging from 0 to the natural resonance frequency; and (*iii*) excitation of the structure with typical operating frequency vibrations for

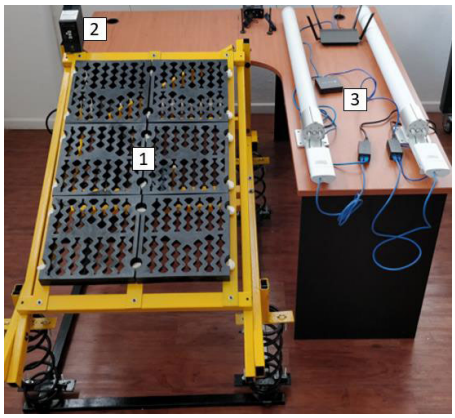

FIGURE 12. Vibratory screener with SmartScreen sensor at lab. Details: (1) Real-size vibratory screens with embedded electronics, (2) Vibration motion control system, and (3) Data networking equipments.

mining applications, i.e. 20 Hz [30]. The natural resonant frequency was obtained by applying FFT transform to the test bench's impulse response over the measurement time record. Catastrophic failures can be induced on the test bench exciting the vibrating screener at resonance frequency and its harmonics [31].

The data-generating process based on experimental testing at lab-scale have some limitations: (*i*) tests are done without load, so equipment condition diagnosis is made over baseline vibratory patterns with higher amplitude excursions; (*ii*) the stiffness and inertia of the test bench deck is lower than real vibratory screener, so scaling factors must be introduced to ensure replication of real operating conditions; (*iii*) the labeling of measured signals is performed matching observed dynamic behavior of the test bench and vibratory stimuli, therefore, to cover typical deviations in the process such as installation defects, loose components, damaged components or missing components, these conditions must be set manually in the test bench. SmartScreen sensors acquire signals at 400 Hz, this means, at 20Hz the typical operating frequency of vibratory screeners.

B. DEM DATA-GENERATING PROCESS

In applications where increasing productivity is desired, maximizing throughput and uptime are the typical focus. In this sense, the equipment must yield a high throughput (i.e. a substantial amount graded granular material) and a high capacity to separate particles into different sizes (that is a high efficiency). To achieve these challenges, a high capacity to early detect unwanted operating conditions in real-time to take predictive and preventive actions is mandatory. Therefore, the analysis of vibrating screen design efficiency under different operating conditions is very important for this purpose. Nevertheless, researching these types of equipment for ways to increase efficiency can be challenging as the mechanisms of particle motion are not fully understood [32].

The parameters can easily be changed in simulations, eliminating the need of preparation, excessive time and resources for the experiments. Also, several tests can be done at the same time. Another great advantage of a computational analysis is the possibility of simulating equipment and systems that does not yet exist, allowing engineers and researchers to decide which solution is better before it is manufactured [32].

When choosing the proper design criteria for monitoring systems for a vibrating screen, an important tool is a parametric analysis. When a vibrating screen operates at high frequencies, it can cause particles to bypass the screen and otherwise not reach the holes in the screen. On the other hand, low frequencies may result in accumulation of the particles on the screen surface, excessive wear, and reduced throughput along the process [32].

If the inclination angle of the screen is too high, the particles could move too fast over the screen and miss opportunities to pass through the screen aperture. If the angle is too low, the particles could accumulate in the screen, which can cause excessive wear and reduced throughput. Low particle mass flow rate in the feeder will result in reduced throughput, which is usually the opposite goal of the process. But if the mass flow is too high, it may cause deformation of the equipment due to higher stress, particle accumulation on the screen and premature wear of the screen [32].

Discrete elements methods (DEM) can be used as modeling tools and data-generating processes to better optimize the process, assisting in the proper selection of these and other design considerations for the development of a new embedded condition monitoring system for vibratory screens. Obtaining correlations between vibrating screen parameters and efficiency may result in valuable insight for industrial equipment O&M improvements and new solution designs [32]–[34].

DEM analysis allows to identify the physical principles that govern a system and develop a numerical model to predict the motion and interactions of particles and domains under different operating conditions [35]–[40].

The software employed in the data-generating proces to provide simulated datasets about material flow, unbalance conditions, and progressive degradation processes for training the machine learning algorithms was Rocky DEM.

Rocky is a powerful 3D Discrete Element Modeling DEM software that quickly and accurately simulates particles' granular flow behavior of different formats and within material processing equipment such as vibratory screens. Rocky allows simulating the transport and handling of materials with particles of various forms with a real size distribution, considering phenomena such as friction, contact, material clogging, rupture, adherence, erosion, and fluid-particle interaction.

The 3D model of the vibratory screener considered for simulations comprises one classification deck with dimensions of 6 [m] $\times$ 3.6 [m], which represents a large-size deck at industrial scale (240 screen panels of 30 $\times$ 30 [cm]). Specifically, the DEM simulation model working as a data-generating process provided the vibratory response, forces, stress levels and wear over the vibratory deck screen under different operating conditions.

TABLE 4. Rocky DEM simulation parameters.

Variable Name	Value
Screen pass percentage	34 [%]
Rolling Resistance factor	0.1 [-]
Particle sizes	76; 45; 21; 19; 12; 10 [mm]
Cumm Particle size distribution	100; 88,84; 53,85; 47,99; 22,36; 17,99 [%]
Average material flow	4000 [tonne/h]
Vibrating screen frequency	20 Hz

The DEM model was tuned using a complete set of operation, geological and mechanical parameters considering information reported in literature and operating practice data for vibratory screeners. Key parameters include the system materials, the screen pass percentage, the material rolling resistance factor, size and distribution of particles, tonnes per hour flow, and vibratory frequency and amplitude.

A summary of DEM simulation parameters are listed in Table 4 with their respective values [41]–[43].

The data-generating process based on DEM simulations considers the following limitations: (*i*) the system response is determined at a fixed operating frequency; (*ii*) the input bulk material flow has a normal distribution; and (*iii*) each simulation accounts for near system step-response.

The vibratory screener was simulated at different operating points up to nominal load (4,000 tonnes per hour). Additional overloading operating conditions were simulated to reproduce transient peak stress over the equipment. Fig. 13 shows the bulk material entry in time for near step-response evaluation in the screener at nominal load for a given volume of material. Fig.14 shows a time-step of the 3D simulation of particle material flow over the vibrating screener during near step-response evaluation. The y-axis was implemented as a fixed constraint to ensure convergence in the simulation model. Results in Fig.15 shown that z-axis vibration signals exhibited greater amplitude excursion than x-axis vibrations as a function of the material flow.

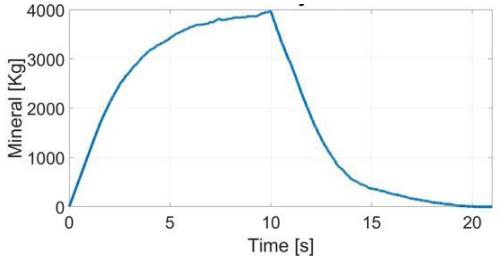

FIGURE 13. Bulk material entry in time for near step-response evaluation in the screener at nominal load for a given volume of material.

Continuous operation of equipment that handles solids causes wear and tear on its components. DEM has proven to be very helful in predicting wear. Before predicting how a surface wears, the forces and stresses that it is subjected to must be accurately computed. In Rocky, the transient variation of

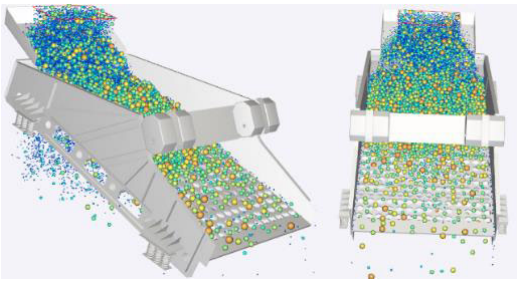

FIGURE 14. View of 3D particle material flow simulation in Rocky DEM.

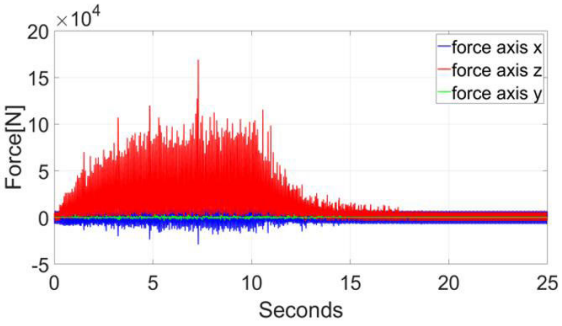

FIGURE 15. View of particle forces acting upon the geometry components of vibratory screener (per axis) as the bulk material flows.

normal and the shear stresses on the surface, and its related work, are computed accurately. Thus, accurate power draw can be used to predict 3D wear evolution. This work uses a validated Archard's wear model in Rocky DEM calibrated against experimental data. This is a shear based model that correlates volume losses in 3D geometry components with the specific work due to friction forces. With calibrated wear rate parameters, this model accurately captures both wear and wear patterns on geometries [44].

Fig.15 shows an example of particle forces acting upon the geometry components of vibratory screener (per axis) as the bulk material flows. The vibratory screens exhibiting more shock impacts are the ones subjected to a more significant wear due to constant vibration and interaction with particles flowing on the Deck. Fig.16 shows a flowchart of the screen wear estimation model implemented for this work based on the vibratory screener's geometry definitions, granulated bulk material parameters and equipment operating conditions.

VI. DIAGNOSTIC ALGORITHMS

A diagnostic algorithm to be developed must decide whether a fault has occurred (fault detection) and which fault has occurred (fault identification) [45]. When conducting exploratory studies with no prior information about data, a supervised learning algorithm can help to predict outcomes for unforeseen data. Supervised machine learning algortihms are designed to learn by example. Supervised learning is the machine learning tasks of learning a function that maps an input to an output based on example input-output pairs.

TABLE 5. Characteristic machine learning algorithms.

ALGORITHM	ADVANTAGES	DISADVANTAGES
Support Vector Machines	Robust and accurate results with large non-linear input. Good generalization performance is guaranteed. They were successfully applied to machinery failure diagnosis. An efficient prediction method for small samples.	There is no standard method for choosing the kernel function of what the key process for SVM is. Difficult to construct a univariate time series for remaining life and sampling time. Parameters must be adjusted explicitly for a problem, and this can be difficult.
Naïve Bayes models	Computes non-linear degradation predictions and solutions to complex regression and classification problems. A flexible non-parametric probabilistic technique offering prediction of uncertainty through the variance around the prediction of the Gaussian process model. It adapts to the environment and learns from experience.	High computational load, especially when training data sets are large Assume that all points are normally distributed and that the error between each point is correlated It isn't easy to find optimal values of the scale parameters Assume that the noise in the training data is constant throughout the input domain.

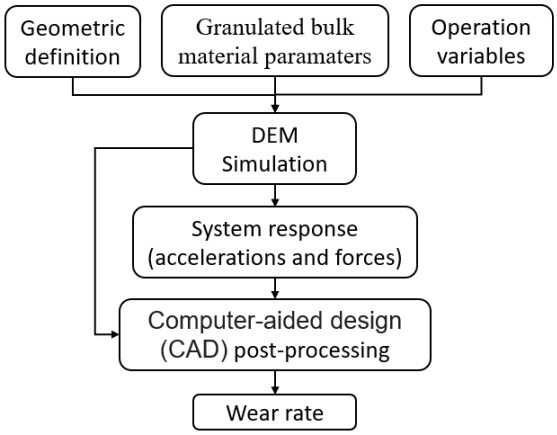

FIGURE 16. Wear estimation methodology.

It infers a function from labeled training data consisting of a set of training examples.

A supervised learning consisting of an input object (typically a vector) and a desired output value (also called a supervisory signal). A supervised algorithm analyzes the training data and produces an inferred function, which can be used for mapping new examples. During training, the algorithm will search for patterns in the data that correlate with the desired outputs. After training, the supervised learning algorithm will take in new unseen inputs and will determine which label the new inputs will be classified as based on prior training data. With this approach, the training is done through an exper's supervision of essential characteristics and attributes of data. Under this scheme, the algorithm's main task is to optimize the parameters of its model.

Supervised machine learning can be split into two subcategories: classification and regression models. First type of techniques are addressed in this work.

Choosing the optimal algorithm for a problem is dependent on features such as speed, forecast accuracy, training time, amount of data required to train the algorithm, how easy is implementation, how difficult is to discuss and explain patterns and algorithms, and most importantly, being confident that the algorithm solves the problem [46].

Table 6 shows the specific requirements for two supervised machine learning techniques selected for this work. These models achieve high accuracy with a moderate amount of data and low computational cost [47].

TABLE 6. Vibration severity label according to ISO 2372 for screen panels for different excitation signals at lab test bench.

ISO 2372 VIBRATION SEVERITY	CONDITION	VIBRATION CONDITIONS
Good	Homogeneous vibration	0.2-0.25g @ 20 Hz
Acceptable	Homogeneous vibration with spurious heterogeneous vibrations	0.3-0.55g ~20 ± 2 Hz
Unsatisfactory	Fully heterogeneous vibrations	0.47-0.83g ~20 ± 4 Hz
Unacceptable	Heterogeneous vibrations with fully unbalanced deck condition	0.6-1.1g ~20 ± 10 Hz

One key issue for most classification algorithms is that they need large amounts of labeled samples to train the classifier. Since manual labeling is time-consuming, researchers have proposed active learning and semi-supervised learning technologies to reduce manual labeling workload. Of numerous SVM active learning algorithms, the most popular is the one that queries the closest to the current classification hyperplane in each iteration. Realizing that SVM active learning is only interested in samples that are more likely to be on the class boundary, while ignoring the usage of the rest large amounts of unlabeled samples, this paper uses an iterative design of semi-supervised learning algorithm to make full use of the rest non-queried samples, and further forms a new active semi-supervised SVM algorithm. The proposed active semi-supervised algorithms use active learning to select class boundary samples and semi-supervised learning to select class central samples. Class central samples are believed to better describe the class distribution and help SVM active learning algorithms finding the boundary samples more precisely. In order to avoid introducing too many labeling errors

when exploring class central samples, the label changing rate is used to ensure the reliability of the predicted labels. Testing with experimental and simulated results showed that the proposed active semi-supervised learning SVM algorithms outperform the pure SVM active learning algorithms, thus reducing manual labeling workload. Figure 17 shows the framework of the active semi-supervised SVM machine learning algorithms used in this work to detect anomalies and predict progressive damage. The framework also was applied to implementing alternative predictive models based on Naïve Bayes algorithms with same purposes [48].

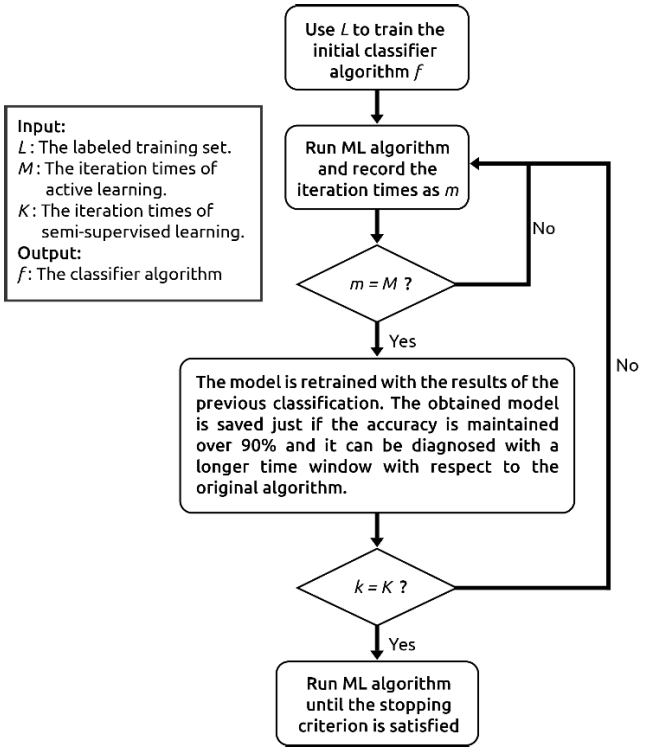

FIGURE 17. Framework of the active semi-supervised machine learning algorithms used in this work [49].

This work explores active learning and semi-supervised learning instead of traditional supervised learning. Semi-supervised learning aims to label unlabeled data points using knowledge learned from a small number of labeled data points. Supervised learning aims to learn a function that, given a sample of data and desired outputs, approximates a function that maps inputs to outputs. In active learning, the algorithm proactively selects the subset of examples to be labeled next from the pool of unlabeled data.

A. ANOMALY DETECTION ALGORITHMS

Anomaly detection, also known as outlier detection, identifies extreme points or observations that significantly deviate from the remaining data. Usually, by analyzing these extreme points, the user can understand the extreme working conditions of the system. In vibratory screeners, some anomalies could be a sudden increase in the vibration severity or unbalance due to surprising increase in material volume flow or unexpected failure of critical components. Proper anomaly detection should be able to distinguish signal from noise to avoid too many false positivies in discovering-malies [50], [51].

Today, a critical issue for developing a vibratory screener data-driven monitoring strategy based on pattern recognition models is the lack of diagnostic labels to explain the measured data. In an engineering context, these descriptive labels are costly to obtain, and consequently, the use of conventional supervised learning is not feasible. Active learning tools look to solve this issue by selecting a limited number of the most informative observations to query for labels. Active learning is motivated by scenarios where it is relatively easy to amass large quantities of data but costly/impractical to obtain their labels. Here, the key philosophy is that a pattern recognition algorithm can achieve greater performance, using fewer training labels if allowed to select the data from which it learns. Like supervised learning, the goal is to ultimately learn a mapping function from the observations to labels. However, here the data are initially unlabeled, more precisely, the algorithm systematically builds an informative training set limited to a budget of given observations [51]–[53].

Correspondingly, the data labeling of the initial data training set is relevant for good active semi-supervised learning. These data labels were generated by measuring vibrations and assessing the test bench screener behavior under a permanent vibrating regime and dynamic response of the test rig to different excitation signals. The frequency sweep test data were measured on the test bench for failure prediction due to abnormal operating conditions like vibrations at resonance frequency (or some of its harmonics). The measuments consisted of 65,500 sample datasets. Each input data sample was composed of 6 variables: vibration RMS value, vibration cumulative RMS value, amplitude of acceleration in the x-y-z axles, and the screen vibratory frequency. Each output corresponded to the vibration severity label according to ISO 2372 standards. See Table 6.

With proposed SmartScreen sensors, conditions like screen panel loose or breakdown can be easily identified thanks to embedded accelerometers. The accelerometer devices are used to measure abnormal acceleration forces. Such forces may be static, like the continuous force of gravity or, as is the case with vibratory screens, dynamic to sense abrupt movements due to failure condition or vibrations in permanent regime. In specific, the motion sensors in accelerometers allow the measurement of the change in velocity and acceleration forces. Surge changes in individual velocity or acceleration force are monitored to trigger failure alarms using fixed thresholds according to the machinery' condition variables for diagnosis.

Other anomaly early-failure detection capabilities like detection of blocking and/or clogging of screen panels and excessive Deck unbalance are implemented using machine learning models. The outlier detection classifiers used in this work correspond to the Naïve Bayes model with kernel density estimation and the quadratic SVM model.

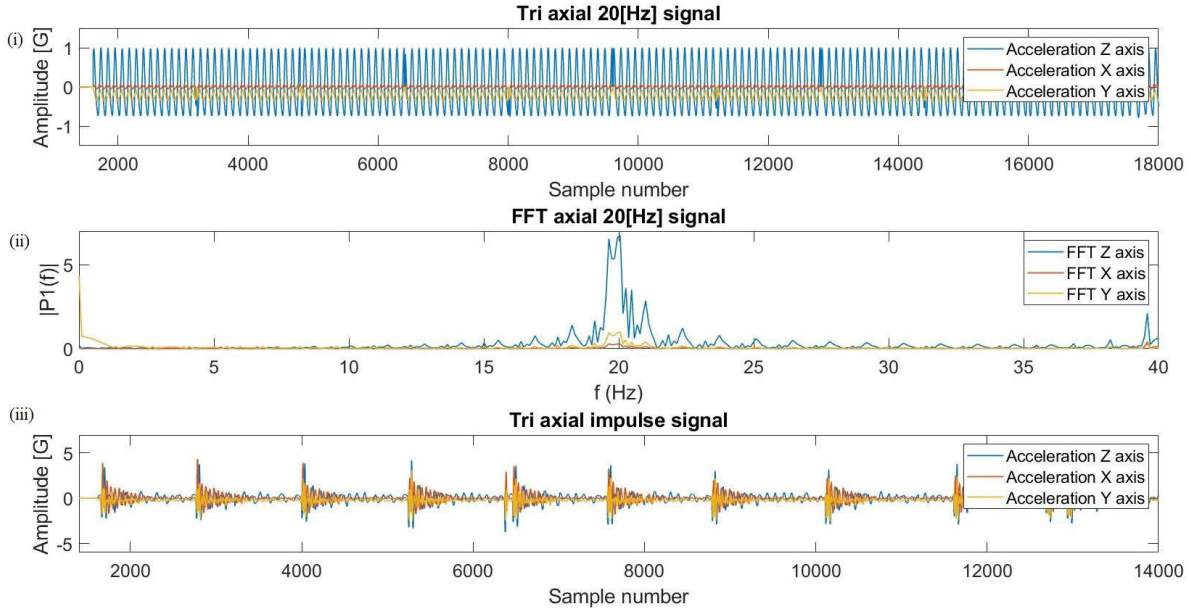

FIGURE 18. Test bench signal, (i) Vibratory excitation triaxial signal at 20 Hz, (ii) Fast fourier transform into (i), (iii) Signal response to impulse excitation.

The 65,500 datasets of vibrating severity labels according to ISO 2372 and vibration measurements collected in test bench under different operating conditions presented the following distribution per class label: 30% Good state, 25% Satisfactory state, 25% Unsatisfactory state, and 20% Unacceptable state. For training, validation and testing, the usage of datasets was 60%, 30% and 10%, respectively. Random selection was used over each vibratory severity dataset.

B. PROGRESSIVE DAMAGE PREDICTION ALGORITHMS

An important problem during vibratory screener operations is the detection and classification of parts wear, specifically, screen panels. Previous research has demonstrated effectiveness of various feature sets and binary classifiers to detect other operating conditions and maintenance problems. Here, the goal is to develop a classifier which makes use of dynamic characteristics of screen panel's wear in a vibratory screener application with two outputs: (*i*) a prediction of the individual screen panel wear level (quantized) and (*ii*) a gradient measure of wear probability given the observed feature sequence. The classifiers proposed in this work track the dynamics of SmartScreen sensor data within each condition monitoring time step andhe evolution of wear from installation to the end of lifespan [54].

Screen panels suffer from progressive wear, which, if not controlled or detected, impairs material classification. If vibratory screens continues operating with worn panels, it will break causing further damage to the vibratory Deck or other downstream equipment. By inspecting the vibratory screener regularly, operators can predict the amount of wear on the screen panels. However, it is not possible to dedicate an expert maintainer to constantly monitoring vibratory screens' wear. What is needed is an automatic system that alerts the operators when close supervision of vibratory screens is required and when screen panels replacement is warranted [54].

A common industrial practice is to replace rubber screen panels according to a fixed schedule based on average lifespan. This approach is innefective because of the wide variation in usage. Past work on automation of vibratory screen panels has treated classification as a binary decision, of not worn versus worn. In this work, we replace this binary decision by a multilevel quantized wear estimate. Furthermore, this work generates a confidence estimate that screen panels have exceeded an acceptable level of wear. The intention is to provide information that allows more timely and accurate decisions about screen panel replacement. In vibratory screens, the wear is a dynamic process, with rubber screen panels moving from being new to progressively greater levels of wear and possibly to breakage. We model the multiple levels of wear assuming a monotonically increasing wear and representing the dynamics of the material screening process. To deal with the problem of sparsely-labeled training data, we propose and evaluate several alternatives for using unlabeled data in estimating model parameters using active semi-supervised learning combined with Naïve Bayes with kernel density estimation and quadratic SVM classifiers [54]–[57].

The simulation results from DEM data-generating process were used for progressive wear prediction model training. Specifically, the 11 discrete wear levels provided by embedded sensors into screen panels were correlated to wear rate and simulations results to generate classification levels. As the rubber screen panel wear increases and gets closer to the inner steel frame, the wear level estimated was labeled as Good up to 6 mm of wear, Acceptable from 6 to 7 mm of wear, Unsatisfactory from 8 to 9 mm of wear, and finally, Unacceptable over 9 mm of wear. Fig.19 shows the reference for measuring the level of wear on each rubber screen panel.

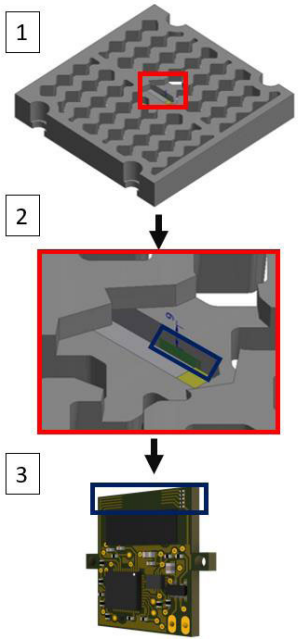

FIGURE 19. Wear estimation rubber screen. (1) Sensor position in rubber screen, (2) Wear sensor section in rubber screen, (3) wear sensor position in electronics embedded system.

The 3,134 datasets of simulated operating conditions and the respective wear level labels used to predict the progressive wear of vibratory screens presented the following distribution per class label: 30% Good state, 25% Satisfactory state, 25% Unsatisfactory state, and 20% Unacceptable state. For training, validation and testing, the usage of datasets was 60%, 30% and 10%, respectively. Random selection also was used over each progressive wear dataset.

VII. RESULTS

This section analyzes the data generated and collected for the bench test and the DEM simulation. The analysis consists of the extraction of characteristics by processing qualitative information (expert observation and trend models) and quantitative information (statistical methods). After the Feature extraction from the data, different classification algorithms are designed and trained to diagnose the status of the screen according to ISO 2372.

A. SmartScreen SENSOR TESTING

The test bench comprises two three rubber screen columns (that composed de SmartScreen). Fig. 20 shows the test bench's reference system.

A vibratory excitation is carried out controlled by the frequency variation of the test bench. The test consists of sweeping frequencies from 5 Hz to 30 Hz in multiples of five. On the z-axis, the signal's maximum amplitude is reached, which is around 3.5 G.

Table 7 shows that the highest peak-peak values are found in the Z-axis, followed by Y and, finally, the X-axis. The "3" and "4" screen has the highest peak-peak values in all axes,

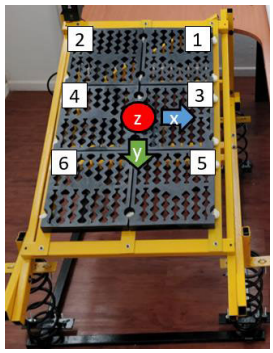

FIGURE 20. Test bench reference system. i) Screen identifier label (from 1 to 6), ii) Inertial sensor reference axis.

TABLE 7. Peak-peak acceleration per screen and axis.

Screen reference	X axis maximum acceleration[G]	Y axis maximum acceleration[G]	Z axis maximum acceleration[G]
1	2.95	3.06	5.68
2	2.93	3.03	5.67
3	3.24	3.29	7.04
4	3.23	3.28	7.04
5	2.27	2.99	5.67
6	2.25	2.98	5.66

followed through the "1" and "2" and ending with the "5" and "6".

The test bench is analyzed in the vibrating screen work frequency (20 Hz). The test result is a sinusoidal signal for each axis. The Z-axis signal has the most significant amplitude, followed by the Y-axis and ending with the X-axis. When applying the FFT in the three axes, a peak at 20 Hz is the forced excitation prints a movement at this frequency in the three reference directions. This can be seen in Fig. 18(i) and Fig. 18(ii).

Applying the FFT to the impulse signal's response, we obtain the resonance frequency 16 Hz. Knowing the test bench's resonant frequency makes it possible to condition unforeseen faults, bringing the operating frequency closer to the resonant frequency's vicinity.

The test of subjecting the test bench to an impulse signal is carried out by hitting the screen's center with a rubber hammer. Fig. 18 (iii) shows the vibrations generated by the impact. The vibratory signal has damping with exponential decay of the amplitude.

B. EM SIMULATION RESULTS

Four simulations are carried with different numbers of tons hours that flow over the Deck, doing simulations of 2,000, 4,000 (nominal load of the simulated screen), 6,000, and 8,000 (overload of the simulated screen) tons per hour. Table 8 shows the maximum and minimum values of the simulation output variables.

The RMS value is calculated as the square root of the sum of the squares of the acceleration signals (one signal for each axis). The maximum RMS values are inversely proportional

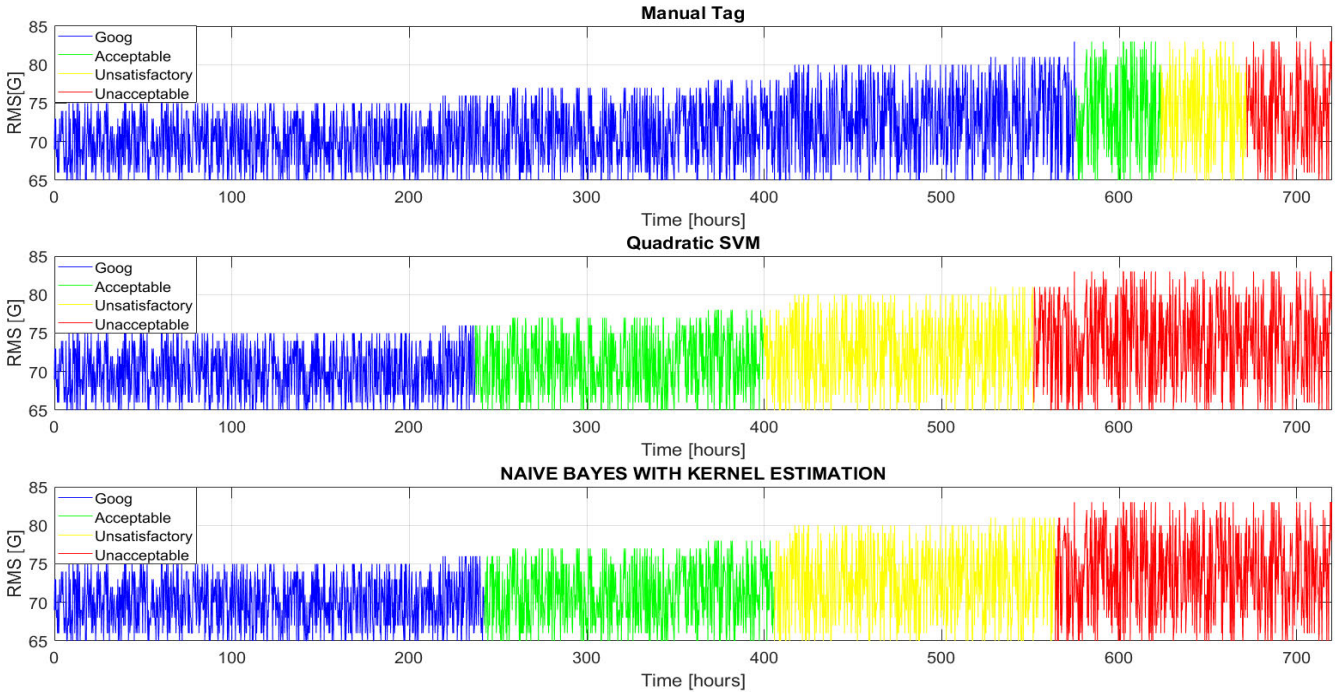

FIGURE 21. (i) Sign labeled by wear level, (ii) SVM tagged signal, (iii) Naïve Bayes tagged signal.

TABLE 8. Maximum and minimum of RMS values and net force.

MATERIAL FLOW T/H	MAX RMS[G]	MIN RMS[G]	Max net force [N]	Min net force[N]
2000	88.8	0.00037	64276	15916
4000	83.1	0.00034	169918	29640
6000	71.6	0.00029	297587	47981
8000	69.28	0.00028	538996	73724

to the tons of flow that pass over the Deck. This behavior is because a greater amount of material flows through the screen, the oscillation amplitude of the Deck decreases.

The maximum and minimum net force values directly proportional to the amount of material flow over the screen. It should be noted that the variability of the maximum and minimum RMS values is around 10% and that the variability of the net forces is about 60%.

Fig. 22 shows the relationship of the different flow levels concerning the cumulative RMS (the sum of the RMS values in a time window). As the mineral flow over the screen increases, the relationship line decreases its slope.

C. ANOMALY DETECTION ALGORITHM(S) TESTING

Table 9 shows the classification results of the tested algorithms (with a k-fold of 15). The test was performed with acceleration RMS value, cumulative RMS, acceleration in the axis X, axis Y, and axis Z. The algorithm has average correct classification of 97.5% and 97.8% for the Naive Bayes algorithms with Kernel estimation and quadratic SVM respectively. For all the algorithms tested, the accuracy in

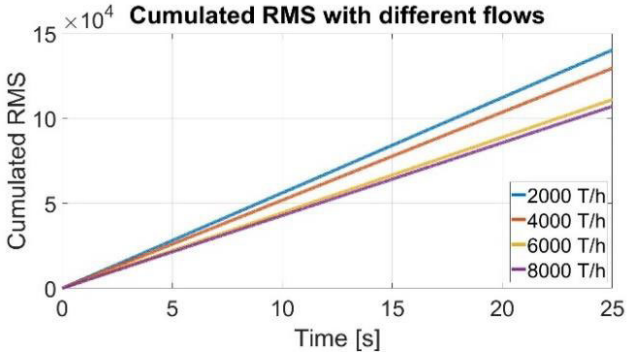

FIGURE 22. Flow levels concerning the cumulative RMS.

TABLE 9. Classification results with all variables.

	NAIVE BAYES WITH KERNEL ESTIMATION	Quadratic SVM
Accuracy Average.	97.5%	97.9%
True positive status "Good".	98%	97.5%
True positive status "Acceptable".	96.9%	98.%
True positive status “Unsatisfactory”.	97.6%	97.9%
True positive status "Unacceptable".	97.9%	98.1%

diagnosing the ‘‘unacceptable’’ state is above the average of the diagnosis of the other states.

Table 10 shows the classification results with a k-fold of 15. This test was performed with the acceleration variables of each axis. The algorithm has a correct classification accuracy

TABLE 10. Classification results with acceleration variables in the 3 axes.

	Naive Bayes with Kernel Estimation	Quadratic SVM
Accuracy average	67.7%	55.9%
True positive status "Good"	91.1%	87.6%
True positive status "Acceptable"	41.8%	25.1%
True positive status "Unsatisfactory"	66.6%	58.2%
True positive status "Unacceptable"	71.1%	72.8%

of 65%, and 55.9% for the Naive Bayes algorithms with Kernel estimation and quadratic SVM.

Table 11 shows the classification results with a k-fold of 15. This test was performed with the variables of RMS and cumulated RMS. The algorithm has a correct classification average of 94.25% and 95.15% for the Naive Bayes algorithms with Kernel estimation and quadratic SVM, respectively. For all the algorithms tested, the accuracy of the ''unacceptable'' state is above average.

TABLE 11. Classification results with RMS variables.

	Naive Bayes with Kernel Estimation	Quadratic SVM
Accuracy average	94.3%	95.2%
True positive status "Good"	92.5%	93.9%
True positive status "Acceptable"	91.9%	92.8%
True positive status "Unsatisfactory"	92.6%	93.9%
True positive status "Unacceptable"	99.8%	99.8%

D. PROGRESSIVE WEAR PREDICTION ALGORITHM(S) TESTING

Table 12 shows that the average classification accuracy is 99.6%. The difference between the two algorithms is the accuracy of classifying the different states. For all algorithms tested, the ''unacceptable'' status accuracy is 99.8%.

TABLE 12. Classifiers with all variables delivered from multiphysics simulation.

	Naive Bayes with Kernel Estimation	Quadratic SVM
Accuracy average	99.1%	99.9%
True positive status "Good"	98.5%	99.9%
True positive status "Acceptable"	100%	99.9%
True positive status "Unsatisfactory"	98.8%	99.5%
True positive status "Unacceptable"	99.8%	99.8%

Table 13 shows the classification results with a k-fold of 15. This test was performed with the acceleration variables of each axis. The algorithm has a correct classification average of 28.9%, and 25% for the Naive Bayes algorithms with Kernel estimation and quadratic SVM.

TABLE 13. Classification with acceleration variables delivered by multiphysics simulation.

	Naive Bayes with Kernel Estimation	Quadratic SVM
Accuracy average	28.9%	26%
True positive status "Good"	49.6%	100%
True positive status "Acceptable"	0%	1%
True positive status "Unsatisfactory"	66.2%	1%
True positive status "Unacceptable"	0%	0%

Table 14 shows the classification results with a k-fold of 15. This test was performed with the variables of RMS and cumulated RMS. The algorithm has a correct accuracy classification of 97.5% and 99.8% for the Naive Bayes with Kernel estimation and SMV quadratic. For all the algorithms tested, the classification of the ''unacceptable'' state is above the average.

TABLE 14. Classification with cumulated RMS and RMS variables delivered by multiphysics simulation.

	Naive Bayes with Kernel Estimation	Quadratic SVM
Accuracy average	95.5%	99.8%
True positive status "Good"	93.9%	99.5%
True positive status "Acceptable"	94.8%	99.9%
True positive status "Unsatisfactory"	95.2%	99.9%
True positive status "Unacceptable"	97.2%	99.9%

The vibratory screen simulated in the present investigation is designed to work with a nominal load of 4,000 tons/hours. In an industrial process, the nominal load is made up of a distribution of different flows. Fig. 20 shows the deck wear rate over time at different flow levels.

A wear rate composed of a normal distribution of flows is estimated. Wear with flow composed of a normal flow distribution takes 30 days to reach the 9[mm] wear level (or unacceptable state). Also, be ruled out that this is limited between the level of wear generated by the flow of 8000 tons hours and the nominal flow. Fig. 23 shows that the Deck's wear at 2000 tons hours is gradual and a resolution of 0.5[mm]. As the flow increases, the homogeneity is lost from 0.5[mm] to 1[mm], accelerating the wear rate.

For maintenance tasks, it is essential to have high accuracy in diagnosing the vibratory screen's operating status and with

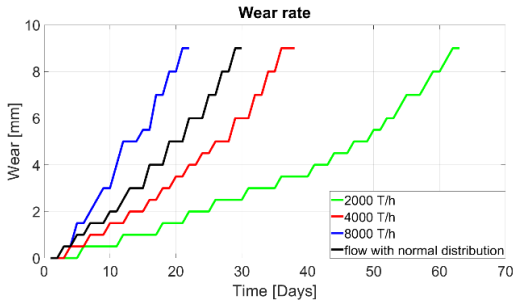

FIGURE 23. Wear rate over time, for different amount of material flow.

TABLE 15. Predictions with semi-supervised models and manual diagnosis.

	Forecast horizon for change in operating status [hours]		
	Acceptable state	Unsatisfactory state	Unacceptable state
Expert Label	144	96	48
Naive Bayes	477	314	156
Quadratic SVM	482	320	168

the greatest amount of time in advance. This paper presents a method for recognizing the operating status.

The method consists of generating a polynomial ($f_a(t)$) composed of the low flow, overflow, and nominal flow signals. Each of these signals is composed of a constant C_n, which $\sum C_n = 1$.

$$f_a(t) = C_1 * f_{low}(t) + C_2 * f_{nom}(t) + C_3 * f_{over}(t) \quad (1)$$

Fig 21. shows the RMS values of the simulation's vibrations (with a normal distribution of flows, that is to say, $C_1 = 0.2, C_2 = 0.6$ *and* $C_3 = 0.2$). According to the level of wear, these signs were labeled, homologated to ISO 2372. The simulation shows a work cycle of 30 days (when the vibratory screen reaches the unacceptable state of wear), with a sample every 15 minutes. Table 15 shows the predictions of the state of health of the semi-supervised machine learning models against the results of the manual diagnosis (diagnosis which was labeled under ISO 2372 according to the level of wear resulting from the multiphysics simulation). The semi-supervised learning process consists of the following steps: (i) the amount of data that exists for each of the four possible states of the model that learned in a supervised way is quantified (79% Good, 7% Acceptable, 7% Unsatisfactory, and 7% Unacceptable), (ii) Then the model under supervised learning is obtained, to which an unlabeled data set is delivered, and it is observed how it classifies them, (iii) with the new labeled data set a new model with a different number of possible states is trained (55% Good, 15% Acceptable, 15% Unsatisfactory and 15% Unacceptable), (iv) if the model trained with the new data set provides a classification accuracy of less than 90%, is discarded. If the model delivers an accuracy greater than 90%, it is analyzed how far in advance concerning manual labeling; it manages to label the signal, (v) if the label's anticipation is less than a range of 96 hours, the model is retrained.

The proposed machine learning models improved over 168 hours forecasting horizon compared to manual wear-based diagnostics delivered by simulation.

VIII. CONCLUSION

A rugged, easy-to-deploy, and smart vibration monitoring system based on IoT devices to assess the real-time conditions of the vibratory screen in the mining industry was successfully developed by providing the cost-effective solutions for hardware, firmware, and machine learning algorithms for the software. The new system is intended to monitor a vibrating screen's operation and notify the users to detect the abnormal operations or faults. This would warn the users of malfunctions and impending failure events before machines become inoperable. Instead of relying on reactionary troubleshooting for maintenance, the vibrating screens would be actively monitored.

The condition monitoring system is specifically optimized for vibratory equipment and, it was tested with two methods. The first method is of tests on a test bench which is subjected to a series of controlled vibratory excitations to characterize its response (without load) both in time and frequency. The data obtained from the test bench suggests a 97.9% precision in the vibratory screen's failure status (according to ISO 2372) using the classified algorithm.

A frequency sweep was carried out to label the vibratory screen's behavior when approaching the natural frequency and its respective harmonics.

The second method corresponds to multiphysics simulations performed in the RockyDem to simulate the vibrational behavior of a screen under different load conditions. The system was able to categorize with a 99.8% precision of the wear of the meshes according to ISO 2372.

This algorithm only uses the DECK's cumulated RMS value obtained as a response from the multiphysics simulation.

When comparing the classification algorithm's result between using all the variables and only using RMS and cumulated RMS value, only a decrease in approximately 2% in the classification accuracy (for both the wear and failure analysis algorithms) was observed. This finding is extremely relevant since due to the limitations of energy storage (due to the maximum size available for the battery), the sending of information can be optimized. Instead of each device sending each of the axes' accelerations' raw data, it is possible to send indicators by time-step. Sending the RMS value and the highest amplitude with its frequency of the signal's FFT, which reduces connection time and device data transfer, processes associated with the highest power consumption.

Concerning the data obtained in the measurement (of the test bench), it is shown that the amplitudes in the collected data have considerable variability against the frequencies. This is consistent with traditional maintenance standards, which estimate equipment's general health with vibration amplitude analysis.

The results suggest that the ratings are sufficient to detect machine condition in real-time, due to good accuracy for both

wear and failure detection (97.5%, 97.9%, respectively) and a high true positive rate (100% for both cases) for the most critical state (''Unacceptable''). Moreover, the system allows early detection of ''Unacceptable'' states between 168 hours before maximum deck wear. These results demonstrate that the proposed system will collect relevant data to generate predictive maintenance plans and avoid unplanned downtimes. The algorithms that were implemented to analyze the tests are presented as an alternative to complement the forecasting models based on experience (currently used in vibratory screen) with models based on Physics and Data. With aiming the improving the estimation of the end of the useful life and allow the appropriate actions to avoid reaching a real failure.

The present research manages to diagnose a vibrating screen's operating status from 168 hours in advance concerning the manual tag based on expert knowledge. Hardware, firmware, and software have a robust all-piece design to withstand the constant vibratory motion.

FUTURE SCOPE

As the future scope, a vibratory screen should be monitored in an industrial environment. For this, a user guide must be developed for operators and maintainers associated with the classification tasks. This guide must contain the SmartScreen installation processes, the system start-up description, and the system's operability and maintainability. The data collected in an industrial environment is expected to fit the models developed in the present investigation. Also, optimization must be performed for the selected classifier to obtain better classification results and select characteristics to simplify the devices' data.

REFERENCES

[1] P. King, ''Size classification,'' in *Modeling and Simulation of Mineral Processing Systems*. Oxford, U.K.: Butterworth-Heinemann, 2001, pp. 81–125.
[2] A. Noble and G. H. Luttrell, ''A review of state-of-the-art processing operations in coal preparation,'' *Int. J. Mining Sci. Technol.*, vol. 25, no. 4, pp. 511–521, Jul. 2015.
[3] M. E. Möbius, ''Size separation,'' in *Principles of Mineral Processing*. Englewood, NJ, USA: Society for Mining, Metallurgy, and Exploration, 2003, p. 54.
[4] R. Ahmad and S. Kamaruddin, ''An overview of time-based and condition-based maintenance in industrial application,'' *Comput. Ind. Eng.*, vol. 63, no. 1, pp. 135–149, 2012.
[5] S. Chakraborty, *Handbook of Offshore Engineering*. Amsterdam, The Netherlands: Elsevier, 2005.
[6] C. Okoh, R. Roy, J. Mehnen, and L. Redding, ''Overview of remaining useful life prediction techniques in through-life engineering services,'' *Proc. CIRP*, vol. 16, pp. 158–163, Jan. 2014.
[7] O. A. Makinde, K. Mpofu, and B. Ramatsetse, ''Establishment of the best maintenance practices for optimal reconfigurable vibrating screen management using decision techniques,'' *Int. J. Qual. Rel. Manage.*, vol. 33, no. 8, pp. 1239–1267, Sep. 2016.
[8] A. M. D. C. Serpa, M. B. Ballina, and E. F. Guerra, ''Análisis de criticidad personalizados,'' *Revista de Inganieira Mecanica*, vol. 12, no. 3, pp. 1–12, 2009.
[9] H. F. M. Robayo and J. C. R. Ortiz, ''Elaboración de un análisis de criticidad y disponibilidad para la atracción x-treme del parque mundo aventura, tomando como referencia las normas, SAE JA1011 Y SAE JA1012,'' Repositorio Institucional Universidad Distrital, Bogotá, Colombia, Tech. Rep., 2017. [Online]. Available: http://hdl.handle.net/11349/7854
[10] M. Minerals, ''Crushing and screening handbook,'' Tampere, Finland, Tech. Rep., 2016. [Online]. Available: https://www.ausimm.com/globalassets/insights-and-resources/minerals-processing-toolbox/metso_handbook_fifth_ed.pdf
[11] D. A. E. Moscoso, ''Modelaciín numérica del comportamiento estructural de harnero vibratorio R-MD, mediante acoplamiento entre el método de elementos finitos y elementos discretos,'' Universidad Tecnica Federico Santamaria, Valparaíso, Chile, Tech. Rep., 2016. [Online]. Available: https://repositorio.usm.cl/handle/11673/23338
[12] S. Bondar, J. C. Hsu, A. Pfouga, and J. Stjepandić, ''Agile digital transformation of system-of-systems architecture models using Zachman framework,'' *J. Ind. Inf. Integr.*, vol. 7, pp. 33–43, Sep. 2017.
[13] D. Gürdür, J. El-Khoury, T. Seceleanu, and L. Lednicki, ''Making interoperability visible: Data visualization of cyber-physical systems development tool chains,'' *J. Ind. Inf. Integr.*, vol. 4, pp. 26–34, Dec. 2016.
[14] S. Vaidya, S. Bhosle, and P. Ambad, ''Industry 4.0—A Glimpse,'' *Proc. Manuf.*, vol. 20, pp. 233–238, Jan. 2018.
[15] P. Zheng, H. Wang, Z. Sang, R. Y. Zhong, Y. Liu, C. Liu, K. Mubarok, S. Yu, and X. Xu, ''Smart manufacturing systems for industry 4.0: Conceptual framework, scenarios, and future perspectives,'' *Frontiers Mech. Eng.*, vol. 13, no. 2, pp. 137–150, Jun. 2018.
[16] E. Ponce, R. Cortes, and C. Valdez, ''Desarrollo de harnero vibratorio,'' Revista Facultad de Ingenieria UT, Antofagasta, Chile, Tech. Rep., 2003.
[17] *Catalogo Mallas, Cribas, Telas Metálicas*, Rivet, Santiago, Chile, 2018.
[18] W. Barry and J. Finch, *An Introduction to the Practical Aspects of Ore Treatment and Mineral Recovery*. Amsterdam, The Netherlands: Elsevier, 2006.
[19] O. A. Makinde, B. I. Ramatsetse, and K. Mpofu, ''Review of vibrating screen development trends: Linking the past and the future in mining machinery industries,'' *Int. J. Mineral Process.*, vol. 145, pp. 17–22, Dec. 2015.
[20] G. Schlemmer, ''Principles of screening and sizing,'' Phoenix, AZ, USA, Tech. Rep., 2016. [Online]. Available: https://www.911metallurgist.com/blog/wp-content/uploads/2016/01/Principles-of-Screening-and-Sizing.pdf
[21] L. Peng, H. Jiang, C. Chen, and D. Liu, ''A review on the advanced design techniques and methods of vibrating,'' Changzhou, China, Tech. Rep., 2018.
[22] K. Mykoniatis, ''A real-time condition monitoring and maintenance management system for low voltage industrial motors using Internet-of-Things,'' *Proc. Manuf.*, vol. 42, pp. 450–456, Jan. 2020.
[23] D. Anderson, J. Jarzynski, and R. F. Salant, ''Condition monitoring of mechanical seals: Detection of film collapse using reflected ultrasonic waves,'' *J. Mech. Eng. Sci.*, vol. 214, no. 9, pp. 1187–1194, Sep. 2000.
[24] A. A. Alkahtani, S. M. Norzeli, and F. H. Nordin, ''Condition monitoring through temperature, vibration and radio frequency emission,'' *Test Eng. Manage.*, vol. 800, pp. 5621–5636, Dec. 2019.
[25] IMI SENSORS, ''Vibratory screens & feeders,'' Marseille, France, Tech. Rep., 2016. [Online]. Available: https://pdf.directindustry.com/pdf/pcb-piezotronics/imi-sensors-vibration-screens-feeders/111589-378823.html
[26] *Screenwatch*, Metso Minerals Industries, Harrisburg, Finland, 2016.
[27] D. Volante, ''Condition monitoring for rotarional machinery,'' Hamilton, ON, Canadá, Tech. Rep., 2011. [Online]. Available: https://macsphere.mcmaster.ca/bitstream/11375/11111/1/fulltext.pdf
[28] E. Willenbrinck, ''Sistema y metodo para la monitorizacion y detecion de anomalias en piezas de materiales polimericos,'' Chile Patent 2021 00 871, Apr. 17, 2021.
[29] R. J. Rafaels, ''Cloud computing: From beginning to end,'' CreateSpace Independent Publishing Platform, Washington, DC, USA, Tech. Rep., 2015.
[30] L. Zhao, Y. Zhao, C. Bao, Q. Hou, and A. Yu, ''Optimisation of a circularly vibrating screen based on DEM simulation and Taguchi orthogonal experimental design,'' *Powder Technol.*, vol. 310, pp. 307–317, Apr. 2017.
[31] I. C. Mituletu, G.-R. Gillich, and N. M. M. Maia, ''A method for an accurate estimation of natural frequencies using swept-sine acoustic excitation,'' *Mech. Syst. Signal Process.*, vol. 116, pp. 693–709, Feb. 2019.
[32] ESSS. *https://rocky.esss.com*. Accessed: Dec. 20, 2020. [Online]. Available: https://rocky.esss.co/blog/evaluating-vibrating-screen-efficiency-by-using-the-discrete-element-method/
[33] M. Daigle and K. Goebel, ''Improving computational efficiency of prediction in model-based prognostics using the unscented transform,'' in *Proc. Annu. Conf. Prognostics Health Manage. Soc.*, 2010, pp. 1–12.
[34] M. Daigle and K. Goebel, ''Multiple damage progression paths in model-based prognostics,'' in *Proc. Aerosp. Conf.*, Mar. 2011, pp. 1–10.
[35] M. M. Quispe, ''Formulación de elementos finitos y elementos discretos,'' Centro de Investigación y Matemáticas, Mexico City, Mexico, Tech. Rep., 2013. [Online]. Available: https://cimat.repositorio institucional.mx/jspui/bitstream/1008/468/1/TE_1523.pdf
[36] Z. Yue-Mina, L. Chu-Sheng, and H. Xiao-Mei, ''Dynamic design theory and application of large vibrating screen,'' *Proc. Earth Planetary Sci.*, vol. 1, no. 1, pp. 776–784, 2009.

[37] M. M. Merino, "Modelación dinámica no lineal de harnero vibratorio considerando inercia del mineral y fuerza del mineral sobre el harnero calculada con elementos discretos," Universidad de Concepcion, Concepción, Chile, Tech. Rep., 2017. [Online]. Available: https://docplayer.es/79864337-Tesis-para-optar-al-grado-de-magister-en-ciencias-de-la-ingenieria-con-mencion-en-ingenieria-mecanica.html
[38] Z. Wang, L. Peng, C. Zhang, L. Qi, C. Liu, and Y. Zhao, "Research on impact characteristics of screening coals on vibrating screen based on discrete-finite element method," *Energy Sour. A, Recovery, Utilization, Environ. Effects*, vol. 42, no. 16, pp. 1963–1976, Aug. 2020.
[39] L. Peng, H. Jiang, X. Chen, D. Liu, H. Feng, L. Zhang, Y. Zhao, and C. Liu, "A review on the advanced design techniques and methods of vibrating screen for coal preparation," *Powder Technol.*, vol. 347, pp. 136–147, Apr. 2019.
[40] B. Ramatsetse, K. Mpofu, and O. Makinde, "Failure and sensitivity analysis of a reconfigurable vibrating screen using finite element analysis," *Case Stud. Eng. Failure Anal.*, vol. 9, pp. 40–51, Oct. 2017.
[41] G. Wang and X. Tong, "Screening efficiency and screen length of a linear vibrating screen using DEM 3D simulation," *Mining Sci. Technol. China*, vol. 21, no. 3, pp. 451–455, May 2011.
[42] L. Zhao, Y. Zhao, C. Liu, J. Li, and H. Dong, "Simulation of the screening process on a circularly vibrating screen using 3D-DEM," *Mining Sci. Technol. China*, vol. 21, no. 5, pp. 677–680, Sep. 2011.
[43] Z. Li, X. Tong, B. Zhou, and X. Wang, "Modeling and parameter optimization for the design of vibrating screens," *Minerals Eng.*, vol. 83, pp. 149–155, Nov. 2015.
[44] ESSS. *https://rocky.esss.com*. ESSS. Accessed: Oct. 2020. [Online]. Available: https://rocky.esss.co/blog/predicting-surface-wear-in-industrial-equipment-using-rocky-dem/
[45] J. Lunze, "Discrete-event modelling and fault diagnosis of discretely controlled continuous systems," *IFAC Proc. Volumes*, vol. 39, no. 5, pp. 229–234, 2006.
[46] A. Kanawaday and A. Sane, "Machine learning for predictive maintenance of industrial machines using IoT sensor data," in *Proc. IEEE Int. Conf. Softw. Eng. Service Sci.*, Nov. 2017, pp. 87–90.
[47] E. Zio, F. D. Maio, and M. Stasi, "A data-driven approach for predicting failure scenarios in nuclear systems," *Ann. Nucl. Energy*, vol. 37, no. 4, pp. 482–491, Apr. 2010.
[48] P. Aqueveque, L. Radrigan, F. Pastene, A. Morales, and E. Guerra, "Data-driven condition monitoring of mining mobile machinery in non-stationary operations using wireless accelerometer sensor modules," *IEEE Access*, vol. 9, pp. 17365–17381, 2021.
[49] Y. Leng, X. Xu, and G. Qi, "Combining active learning and semi-supervised learning to construct SVM classifier," *Knowl.-Based Syst.*, vol. 44, pp. 121–131, May 2013.
[50] A. Lavin and S. Ahmad, "Evaluating real-time anomaly detection algorithms—The numenta anomaly benchmark," in *Proc. IEEE 14th Int. Conf. Mach. Learn. Appl. (ICMLA)*, Miami, FL, USA, Dec. 2015, pp. 38–44.
[51] L. Bull, K. Worden, G. Manson, and N. Dervilis, "Active learning for semi-supervised structural health monitoring," *J. Sound Vib.*, vol. 437, pp. 373–388, Dec. 2018.
[52] P. Dangeti, *Statistics for Machine Learning: Techniques for Exploring Supervised, Unsupervised, and Reinforcement Learning Models With Python and R*. Birmingham, U.K.: Packt, 2017.
[53] N. N. Pise and P. Kulkarni, "A survey of semi-supervised learning methods," in *Proc. Int. Conf. Comput. Intell. Secur.*, Dec. 2008, pp. 30–34.
[54] R. K. Fish, M. Ostendorf, G. D. Bernard, and D. A. Castanon, "Multilevel classification of milling tool wear with confidence estimation," *IEEE Trans. Pattern Anal. Mach. Intell.*, vol. 25, no. 1, pp. 75–85, Jan. 2003.
[55] J. A. K. Suykens, "Nonlinear modelling and support vector machines," in *Proc. 18th IEEE Instrum. Meas. Technol. Conf. Rediscovering Meas. Age Informat. (IMTC)*, May 2001, pp. 287–294.
[56] C. Campbell and Y. Ying, *Learning With Support Vector Machines*, vol. 5, no. 1. San Rafael, CA, USA: Morgan & Claypool, 2011, pp. 1–95.
[57] A. Rottmann and W. Burgard, "Learning non-stationary system dynamics online using Gaussian processes," in *Proc. Joint Pattern Recognit. Symp.*, 2010, pp. 192–201.
[58] D. An, N. H. Kim, and J.-H. Choi, "Practical options for selecting data-driven or physics-based prognostics algorithms with reviews," *Rel. Eng. Syst. Saf.*, vol. 133, pp. 223–236, Jan. 2015.
[59] M. Daigle, B. Saha, and K. Goebel, "A comparison of filter-based approaches for model-based prognostics," in *Proc. IEEE Aerosp. Conf.*, Mar. 2012, pp. 1–10.
[60] M. F. Huber, "Recursive Gaussian process regression," in *Proc. IEEE Int. Conf. Acoust., Speech Signal Process.*, Vancouver, BC, Canada, May 2013, pp. 3362–3366.
[61] SKF. (May 2018). *SKF Vibration Sensors Catalog*. Accessed: Mar. 1, 2021. [Online]. Available: https://www.skf.com/binaries/pub12/Images/0901d196804926fe-11604_16-EN-Vibration-Sensor-Catalogue—OK_tcm_12-267858.pdf
[62] CONiQ. (2021). *CONiQ Cloud*. Accessed: Mar. 1, 2021. [Online]. Available: https://www.schenckprocess.com/data/en/files/1107/coniq-cloud-brochure-final-2021.pdf
[63] MEtso. (2021). *Directindustry.com*. Accessed: Mar. 1, 2021. [Online]. Available: https://pdf.directindustry.com/pdf/metso-automation/screenwatch-screen-monitoring/7017-597920-_3.html

PABLO AQUEVEQUE (Member, IEEE) was born in Santiago, Chile, in 1976. He received the B.S. degree in electronics engineering and the Ph.D. degree from the University of Concepción, Concepción, Chile, in 2000 and 2008, respectively. He is currently a Professor with the Department of Electrical Engineering, University of Concepción. He is also the Director with the Center for Industry 4.0 (C4I), Engineering Faculty, Universidad de Concepción. His research interests include bioelectronics, embedded electronic, electrochemical process, power electronics, and wireless power transfer.

LUCIANO RADRIGAN (Student Member, IEEE) was born in Chillan, Biobio, Chile, in 1991. He received the B.S. degree in electronic engineering and the M.S. degree in electrical engineering from the University of Concepción, in 2019 and 2020, respectively, where he is currently pursuing the Ph.D. degree with the Department of Electrical Engineering, Faculty of Engineering.

He currently works at the Center for Industry 4.0, University of Concepción, where applied research is carried out for industrial processes. His research interests include sensors for condition monitoring, the IoT, industrial sensorization, machine learning, energy harvesting systems, embedded systems, and wireless energy transfer.

ANIBAL S. MORALES (Member, IEEE) was born in Concepción, Chile, in 1983. He received the B.S. degree (Hons.) in electronics engineering and the Ph.D. degree in electrical engineering from the University of Concepción, Concepción, in 2004 and 2012, respectively. He is currently an Assistant Professor with the Department of Electrical Engineering, Universidad Católica de la Santísima Concepción, Concepción. His current research interests include power converters, high-current rectifiers, multiphysics FEM modeling, energy efficiency, electrical safety, energy harvesting and technology for mining industry, copper electrowinning, and electrorefining.

EDUARDO WILLENBRINCK is currently the General Manager at Willenbrinck y Cía. Ltda, a company with more than 60 years of experience in the rubber market, he is at the forefront of technology, innovation, and engineering in the elaboration of industrial components tailored to the client for mining, aeronautics, and fuels. The company has important recognitions, such as the National Competitive Management SME Award.